Structural Engineering and Mechanics, *Vol. 49, No. 1 (2014) 129-145*
DOI: http://dx.doi.org/10.12989/sem.2014.49.1.129

Experimental investigation of characteristics of torsional wind loads on rectangular tall buildings

Yi Li[1a], J.W. Zhang[2] and Q.S. Li[*1,2]

[1]*College of Civil Engineering, Hunan University, Changsha, 410082 Hunan, China*
[2]*Department of Civil and Architectural Engineering, City University of Hong Kong, Kowloon, Hong Kong*

(Received May 22, 2013, Revised December 10, 2013, Accepted December 12, 2013)

Abstract. In order to investigate the characteristics of torsional wind loads on rectangular tall buildings, five models with different rectangular cross-sections were tested in a boundary wind tunnel. Based on the test results, the RMS force coefficients, power spectrum densities as well as vertical correlation functions of torsional wind loads were analyzed. Formulas that took the side ratio as parameters were proposed to fit the test results above. Comparisons between the results calculated by the formulas and the wind tunnel measurements were made to verify the reliability of the proposed formulas. An simplified expression to evaluate the dynamic torsional wind loads on rectangular tall buildings in urban terrain is presented on basis of the above formulas and has been proved by a practical project. The simplified expressions as well as the proposed formulas can be applied to estimate wind-induce torsional response on rectangular tall buildings in the frequency domain.

Keywords: rectangular tall buildings; wind tunnel test; RMS torque coefficients; power spectrum density; vertical correlation function; torsional wind loads

1. Introduction

Along wind loads and across wind loads have been of concern to wind engineering researchers and structural engineers for a long time (Davenport 1967, Saunders and Melbourne 1975, Kareem 1982). However, with the development of measurement technology, researchers found that torsinoal wind loads should not be ignored. Displacement and acceleration near the peripheries of tall buildings can be enlarged by wind-induced torsional vibration. Meanwhile, habitants in tall buildings are more sensitive to torsional motion than translation motion (Tallin and Ellingwood 1984).Unlike along wind loads or across wind loads, the mechanism of torsional wind loads is very complex. Boggs *et al*. (2000) identified some common sources of torsional wind loads in a practical project, including building shape, interfering effects of nearby buildings, and dynamic characteristics of the structure frame. Kareem (1981) presented an outline for the development of torsional wind loads on a rectangular cross-section building in frequency domain. Isyumov and Poole (1983) examined the anatomy of the wind induced torsional moments on buildings of square and rectangular cross-section and found the vortex shedding on the back face can provide an

∗Corresponding author, Professor, E-mail: bcqsli@cityu.edu.hk
[a]Ph.D., E-mail: liyi1986@hnu.edu.cn

http://www.techno-press.org/?journal=sem&subpage=8 ISSN: 1225-4568 (Print), 1598-6217 (Online)

important contribution to the dynamic torque. Tallin and Ellingwood (1985) examined the relation between the spectra of base torque and generalized torques experienced by tall buildings. Katagiri *et al*. (2006) divided the local torsional moments acting on rectangular high-rise building into 4 parts which are composed of windward wall, leeward wall, windward and lee side of the side wall and clarified the characteristics of torsional moment on the 4 parts. Li (2000) estimated three components of wind-induced response of a tall building by structural dynamic analysis based on simultaneous measurements in a boundary layer wind tunnel. Liang *et al*. (2004) investigated wind-induced dynamic torque on rectangular cylinders with various side ratios and presented a mathematical model for evaluation of torsional dynamic wind loads.

As we all known, rectangular cross-sectional tall buildings are the most common buildings all over the world for their simple construction and structural safety. Therefore, investigation of characteristics of torsional wind loads on rectangular tall buildings is very significant. In this paper, five models with different rectangular cross-sections were tested by pressure measurements and high-frequency base balance (HFBB) in a boundary layer wind tunnel to study the characteristics of torsional wind loads on rectangular tall buildings. First, the RMS torque coefficients at nine layers on each model were analyzed, the RMS torque coefficients are formulated by use of the (NLSM) none linear least-squares method. Then, power spectrum densities (PSDs) of torque on rigid models were obtained from (fast fourier transform) FFT of time histories of torque coefficients. Comparisons between pressure measurement and HFBB were made to verify the accuracy of the test results and the feasibility of proposed formulas about PSD. Vertical torque correlation coefficients were also discussed and formulated. Finally, dynamic torsional wind loads and wind-induced response of a practical project were respectively calculated by the simplified expression based on above proposed formulas and directly by the pressure results from wind tunnel test, the comparisons between the two methods show a good match, thus verifying the reliability and applicability of the simplified expression.

2. Wind tunnel tests

The tests were carried out in a boundary layer wind tunnel at Hunan University, China. The wind tunnel has a working section of 20m long with a cross-section of 3.0 m×2.5 m. Spires and roughness elements were used to simulate the boundary layer wind flow specified in the Loads Standard Code of China (GB50009-2012 2012) as exposure category C. This urban terrain type specifies a mean wind speed profile with a power law exponent of α=0.22 and a gradient height of 450m.The vertical distributions of mean wind speed and turbulence intensity at various heights over the test section at a scale of 1:500 are illustrated in Fig. 1. The turbulence intensity at the top of model is almost 12.8%, the longitudinal velocity spectrum of the simulated boundary layer flow agrees with the Karman type spectrum well, as shown in Fig. 2.

Five scale models (1:500) with different rectangular cross-section were tested for study. The height of all the models is 0.6 m. There are nine measurement layers on the surface of each model, as shown in Fig. 3(a). The pressure taps were distributed as shown in Fig. 3(b)~Fig. 3(f) to measure the torsional wind loads.

The wind velocity at gradient height for all the wind tunnel tests is 12 m/s. Electronic pressure scanning modules made by Scanivalve Inc. (USA) were used to measure instantaneous fluctuating pressures. The data sampling frequency was set to be 312.5 Hz and the sampling length was 32 s, implying that the total number of the data obtained from a pressure tap is 10,000 at each wind direction.

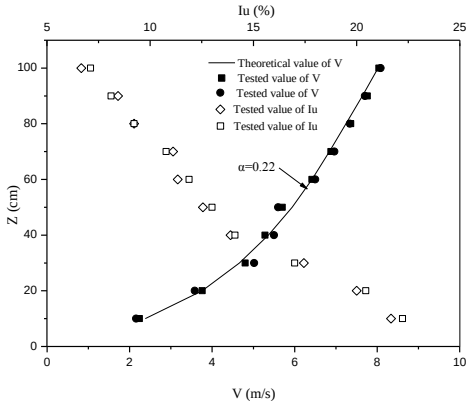

Fig. 1 Mean wind speed and turbulence intensity profiles

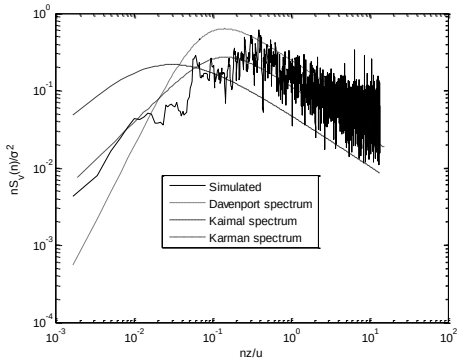

Fig. 2 PSD of longitudinal velocity at reference height

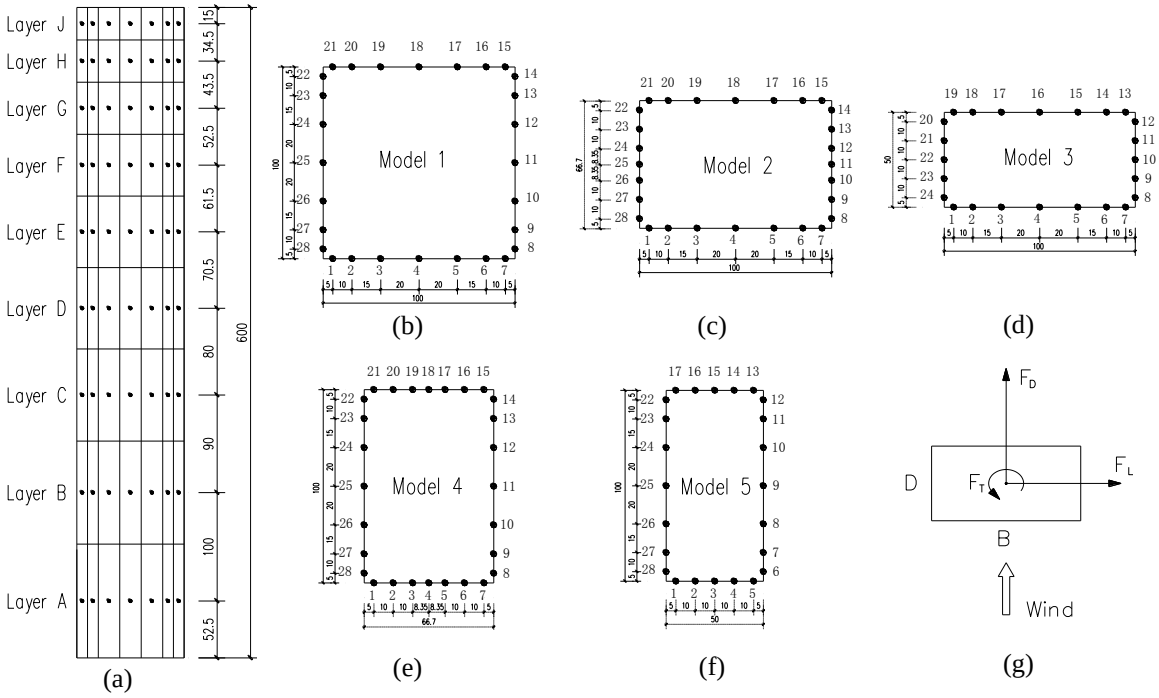

Fig. 3 Measurement configurations: (a) measurement layers, (b)～(f) distribution of pressure taps, (g) definitions of wind loads

Wind loads acting on the buildings are treated as a multiple stochastic stationary Gaussian process characterized by three action components per unit length, referred to the geometric center of the building section: two horizontal forces F_D and F_L acting respectively along and across wind direction, and a torsional moment F_T acting around geometric center (Fig. 3(g)). In Fig. 3(b) B

stands for the breadth of a model in the direction perpendicular to the wind and D stands for the depth.

3. Results and discussions

3.1 RMS torque coefficient

Since the mean force coefficients for torsional direction are close to zero (Lin *et al*. 2005, Gu *et al*. 2009), only the RMS torque coefficients are presented in the study. The RMS torque coefficients at each layer can be defined as follows

$$C_{F_T}(z_i) = \frac{\sigma_{F_T}(z_i)}{P_{\mathrm{Re}f}^H L_i B^2} \tag{1}$$

in which, $\sigma_{F_T}(z_i)$ is RMS of torque at the ith layer; $P_{\mathrm{Re}f}^H = 0.5\rho U_H^2$ stands for the reference wind pressure, ρ is the air mass density, generally considered to be 1.25 kg/m^3, U_H is mean velocity at the top of the model; L_i represents the occupied height of the ith layer, $\sum_{i=1}^{N} L_i = H$, N is the layer of wind force which is equal to nine in the study; B is the width of windward side.

The RMS torque coefficients vary with the side ratio D/B as well as elevation, as shown in Fig. 4. When $D/B \leq 1$, the RMS torque coefficients decrease as the layer height increases; When $1 < D/B \leq 2$, the RMS torque coefficients first increase and then decrease as the layer height increases, the maximum value is less than 0.15 and appears at almost 0.67 H. If we just consider the side ratio, it can be found that the RMS torque coefficients corresponding to the side ratio D/B = 1 is the smallest, while the RMS torque coefficients corresponding to the side ratio D/B = 2 is the largest.

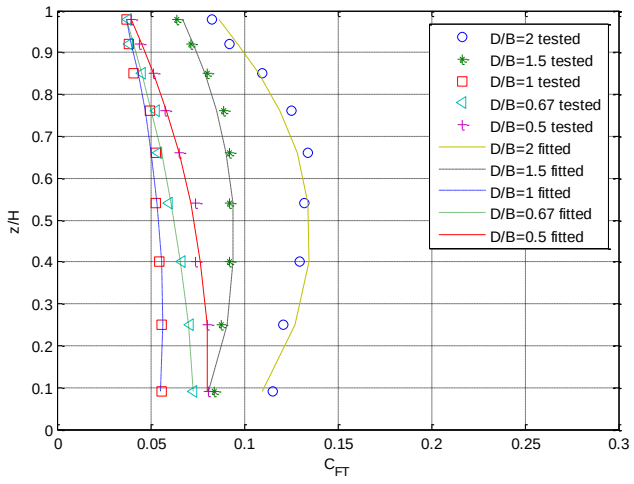

Fig. 4 RMS torque coefficients at each layer

Table 1 The fitted values of the parameters

Parameters	a_1	a_2	a_3
$p1$	5.0425	3.5933	3.9700
$p2$	−4.8791	−3.4712	−3.8664
$p3$	5.6206	4.1968	4.3542
$p4$	−0.9672	−0.7014	−0.5869
$p5$	−0.1098	−0.0475	−0.0681

By applying the nonlinear least-squares method to fit the measured RMS torque coefficients, an empirical formula for $C'_{F_T}(z)$ at different height is obtained as follows

$$C'_{F_T}(z) = a_1 + (a_2 - a_1)(\frac{z}{H}) + (a_3 - a_2)(\frac{z}{H})^2 \tag{2}$$

in which, a_1, a_2 and a_3 are parameters changed with side ratio *D/B*.

$$a_i = p1 + p2(\frac{D}{B}) + p3(\frac{D}{B})^{0.5}\ln(\frac{D}{B}) + p4\ln(\frac{D}{B}) + p5(\frac{D}{B})^{-2}\ i = 1,2,3 \tag{3}$$

Comparison of $C'_{F_T}(z)$ between the results obtained from the wind tunnel test and calculated by the empirical formulas is presented in Fig. 4. The maximum error of the comparison is less than 6%, indicating the predictions based on the empirical formulas match with the test results well.

The RMS coefficients of base torsional moment are very essential to calculate wind-induced torsional response. Many scholars and institutes have provided different empirical formulas for the RMS coefficients of base torsional moment (Marukawa and Ohkuma 1996, AIJ Recommendation for Loads on Building 2004, Ha *et al*. 2008). Comparison of results between the given formulas and the wind tunnel test is shown in Fig. 5. It can be found that all the proposed formulas regard the RMS coefficients of base torsional moment as a function of side ratio *D/B*, and think they increase as the side ratio increases. However, the test results show that the RMS coefficients of base torsional moment first decreases with the side ratio up to 1.0, then increases as the side ratio increases from 1.0 to 2.0. This trend agrees well with the RMS torque coefficients at layers and keeps consistent with conclusions in literature (Zhou *et al*. 2003). The high symmetry of the square model may lead to this phenomenon. What's more, the RMS coefficients of base torsional moment are almost larger than the AIJ or GBJ proposed, especially when the side ratio $D/B \leq 1$, this may cause insecurity to calculate the wind-induce torsional response.

3.2 Power spectra density

The power spectra density of torque is considerably sensitive to side ratio rather than slenderness ratio (Tang *et al*. 2009). Power spectra of torque were obtained for nine layers and the basement on each model. Those at typical layers and the basement are presented to discuss the effects of elevation and building geometry. Fig. 6 present the torque spectra of different models.It can be found that the trend that torque spectra of the basement varied with reduced frequency is almost the same as the torque spectra of each layer at different models. When *D/B*<1, narrow-band peak emerges in the torque spectra, reduced frequencies corresponding to the peaks are lower than

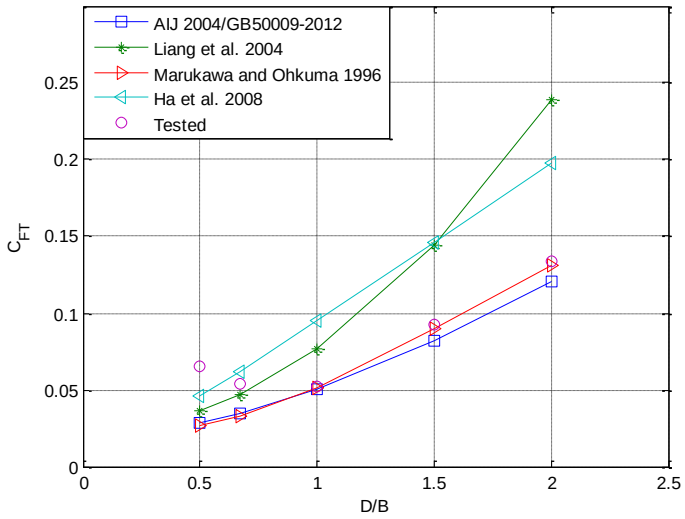

Fig. 5 Comparisons of RMS values of base torque

the Strouhal number (0.1) of rectangular buildings. Turbulence from windward and vortex shedding on the leeward are the main contribution to the dynamic torque. As the side ratio *D/B* increase from 0.5 to 0.67, the peak value decreases and the bandwidth increases, contribution from the side-wall fluctuating increases, thus resulting in the reduced-frequency peak shifts towards Strouhal number. When *D/B*=1, energy of vortex shedding from the leeward and windward of side wall weakened, resulting in the reduction of the Strouhal number component (Katagiri *et al*. 2006). There are two peaks appeared in the torque spectra. The reduced frequency of first peak is close to Strouhal number, though the peak value is lower than those of *D/B*<1. The second peak occurs at a higher reduced frequency which is almost 1.95 times of the Strouhal number, this is caused by the reattachment of the separated flow on the lee side of the side wall. As the side ratio *D/B* continues to increase, the first peak value decreases and the second peak value increases, and the reduced frequencies corresponding to the peaks approach to each other. This implies that the influence of the reattachment begins to amplify and the influence of the vortex shedding gradually reduces.

Differences between non-dimensional spectrum of torque at each layer and non-dimensional base torque spectrum so slight that non-dimensional base torque spectrum can be used to evaluate non-dimensional spectrum of torque at each layer. Power spectrum of base torque is very important for studying torsional wind loads on buildings. Compared with along-wind and across-wind loads, researches on power spectrums of base torque is very rare for its complicacy. Liang *et al*. (2004) proposed two empirical formulas to calculate the base torque spectrum for various side ratios by fitting the experimental data. Tang *et al*. (2009) used the nonlinear least-squares method to fit the power spectrum density of torsion moment as a function of side ratio and terrain category condition. However, the formulas proposed by them are too difficult to apply in practical projects. Marukawa *et al*. (1992) suggested an expression for the power spectra density of the across-wind overturning moments, it can thoroughly reflect the basic characteristics of spectrum of across-wind. The expression takes the vortex shedding and reattachment of separated flow on side-wall into consideration, and be adopted by AIJ Recommendations for its simpleness and feasibility. It can be found from the analysis of PSDs of base torque varied with

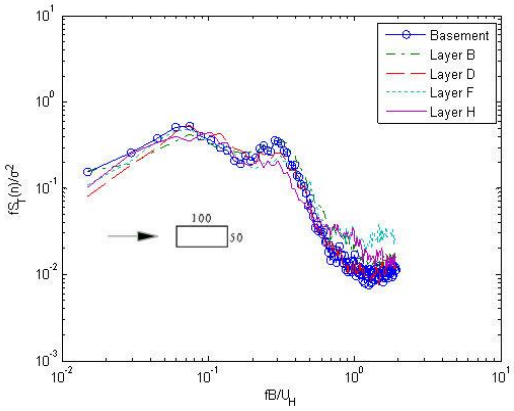

(a) *D*/*B*=2

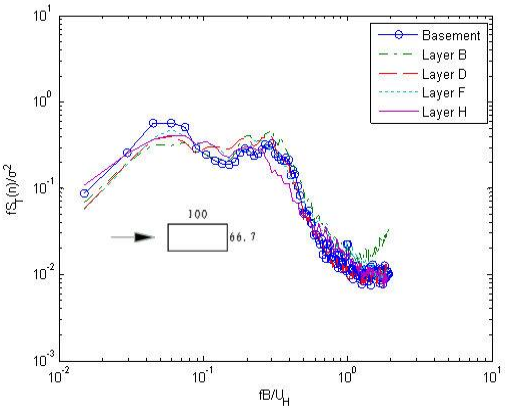

(b) *D*/*B*=1.5

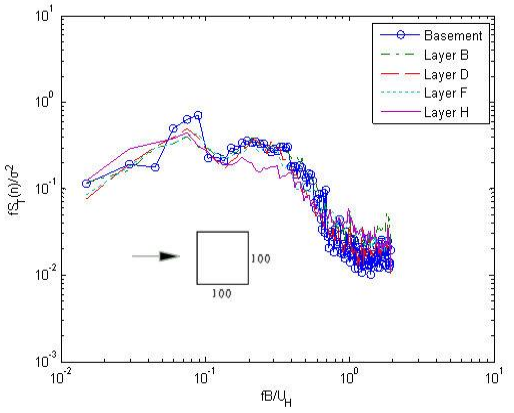

(c) *D*/*B*=1

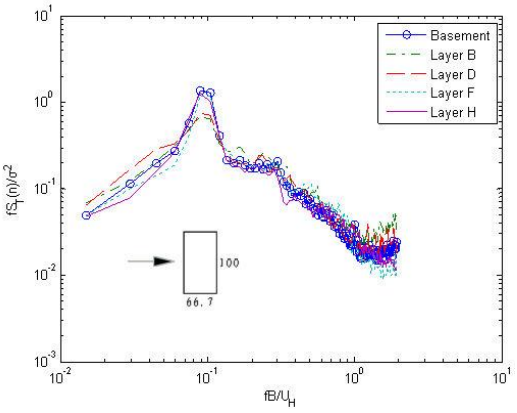

(d) *D*/*B*=0.67

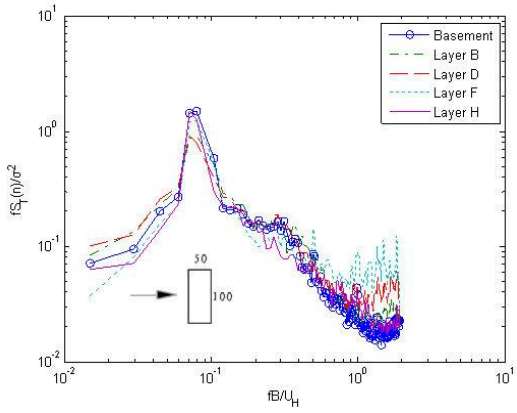

(e) *D*/*B*=0.5

Fig. 6 Torque spectra of different models

side ratios that three components contribute to the total dynamic torque: turbulence from windward, vortex shedding and reattachment of separated flow. Characteristics of vortex shedding

and reattachment of separated flow can be well displayed by the expression proposed by Marukawa *et al*. (1992). Regarding to the turbulence from windward, quasi-steady assumption can be utilized to consider its influence. Based on the above discussion, the following normalized formula is proposed by fitting to the wind tunnel results

$$\frac{fS(f)}{\sigma^2}=\frac{af}{(1+bf^c)^d}+\sum_{j=1}^{N}\frac{K_j(f/F_j)^2}{\left[1-(f/F_j)^2\right]^2+4P_j^2(f/F_j)^2} \tag{4}$$

in which, the first item $\frac{af}{(1+bf^c)^d}$ represents the contribution of turbulence from windward; in the second item $\sum_{j=1}^{N}\frac{K_j(f/F_j)^2}{\left[1-(f/F_j)^2\right]^2+4P_j^2(f/F_j)^2}$, j=1 represents the contribution of vortex shedding while j=2 represents the contribution of reattachment of separated flow.

K_j, P_j, and F_j, a, b, c, d in Eq. (4) are parameters changed with side ratio D/B and can be calculated by following equations

$$K_1=0.506-0.547\cos(2.418-3.16\times\frac{D}{B}) \tag{5}$$

$$K_2=0.449+0.684\cos(6.306-4.179\times\frac{D}{B}) \tag{6}$$

$$B_1=(0.252\times\frac{D}{B}-0.233)/(1-1.129\times(\frac{D}{B})^{-0.95}) \tag{7}$$

$$B_2=(0.014-0.017\times\frac{D}{B})/(1-0.875\times(\frac{D}{B})^{-0.30}) \tag{8}$$

$$F_1=-0.983-1.283\times\frac{D}{B}\times\ln(\frac{D}{B})+0.382\times(\frac{D}{B})^2 \tag{9}$$

$$F_2=-3.774-4.312\times\frac{D}{B}\times\ln(\frac{D}{B})+1.358\times(\frac{D}{B})^2 \tag{10}$$

$$a=16.392-20.698\times\frac{D}{B}+6.208\times(\frac{D}{B})^2 \tag{11}$$

$$b=1/(0.162-0.332\times\frac{D}{B}+0.178\times(\frac{D}{B})^3) \tag{12}$$

$$c=-2.021\times\frac{D}{B}/(\frac{D}{B}-1.976) \tag{13}$$

$$d=(\frac{D}{B}-0.484)/(0.245\times(\frac{D}{B})-0.057)-1.62 \tag{14}$$

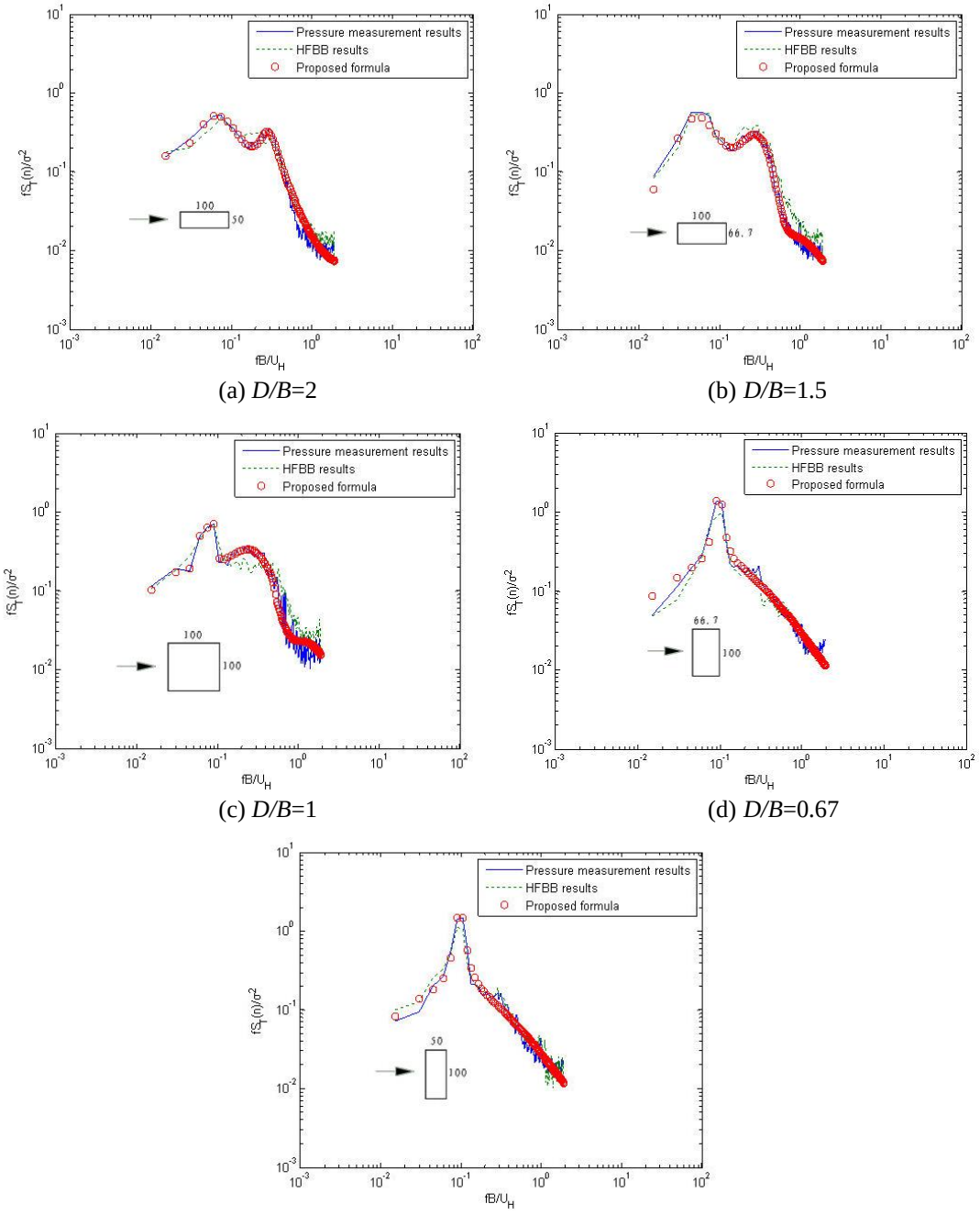

(a) *D*/*B*=2 (b) *D*/*B*=1.5

(c) *D*/*B*=1 (d) *D*/*B*=0.67

(e) *D*/*B*=0.5

Fig. 7 Comparison of torque spectra between the proposed formulas and wind tunnel tests

In order to assess the reliability of the data acquired by the pressure measurement, HFFB method was used to evaluate the spectra of the global forces acting at the base of the building in

the same wind field. The principle of HFFB can be referred to literature (Kown *et al*. 2008). The models used for the HFFB and the pressure measurement were the same at geometrical shape. The models for HFFB were made of light pine wood with internal foam plastic so that they can be regarded as rigid models. The comparisons of base torque spectrum between wind tunnel tests including the pressure measurement as well as the HFFB method and the proposed formula are shown in Fig. 7. The results show that base torque spectrum acquired by the two techniques agree well with each other. Meanwhile, the proposed formulas can be used to evaluate the base torque spectrum effectively.

3.3 Vertical correlation coefficients

The correlation coefficients represent the mutual dependence of two random variables. Vertical correlation at different height is concern of wind engineers. The vertical correlation coefficients of fluctuating torsion $Cor_{F_T}(z_i, z_j)$ are defined as follows

$$Cor_{F_T}(z_i, z_j) = \frac{Cov_{F_T}(z_i, z_j)}{\sigma_{F_T}(z_i)\sigma_{F_T}(z_j)} \tag{15}$$

in which, $Cov_{F_T}(z_i, z_j)$ is covariance of torsion between height z_i and z_j, $\sigma_{F_T}(z_i)$ and $\sigma_{F_T}(z_j)$ is respectively mean square error of height z_i and z_j.

As shown in Fig. 8, as the side ratios *D/B* increases, correlation coefficients of the adjacent layers at base or top of the models gradually decrease. When *D/B*<1, correlation coefficients of the adjacent layers at upper half stay around 0.3~0.4. When *D/B*>1, correlation coefficients of the adjacent layers rapidly decrease as the relative height increases. On the basic of that the non-dimensional spectra of the base torque is approximately equal to those of the different layers, vertical coherence function is equivalent to vertical correlation coefficient, both of which are functions irrelevant with frequency (Tang 2006). Vickery and Clark (1972) thought wake excitation contributed most in dynamic torque and proposed a vertical coherence function of wake excitation, but the parameters in function is only available for some fixed side ratios. Based on the test results, a new function varied with different side ratios has been presented as follows

$$Cor_{F_T}(z_i, z_j) = a \times \exp^{(-bx)^2} \tag{16}$$

In which, $x=|z_i-z_j|/H$; *a*, *b* are parameters varied with side ratios and can be determined as follows

$$a = 36.89 + 3.22(\frac{D}{B}) - 18.63\ln(\frac{D}{B}) - 47.60(\frac{D}{B})^{-0.5} + 8.40(\frac{D}{B})^{-1} \tag{17}$$

$$b = 17.67 + 7.70(\frac{D}{B})^{2.5} - 7.69 \times \exp(\frac{D}{B}) - 2.51(\frac{D}{B})^{-1} \tag{18}$$

The curves in Fig. 8 display the fitting results of the formulas. Vertical correlation coefficients calculated by the formulas keep good consistent with test results, indicating the formulas possess high accuracy and can represent the rules vertical correlation coefficients changed with side ratio very well.

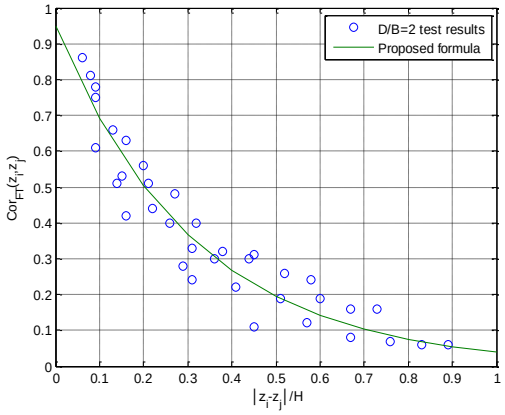

(a) *D*/*B*=2

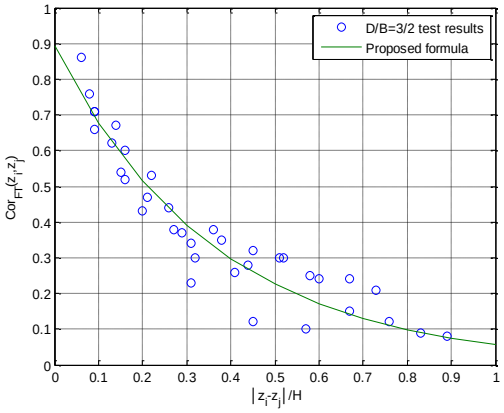

(b) *D*/*B*=1.5

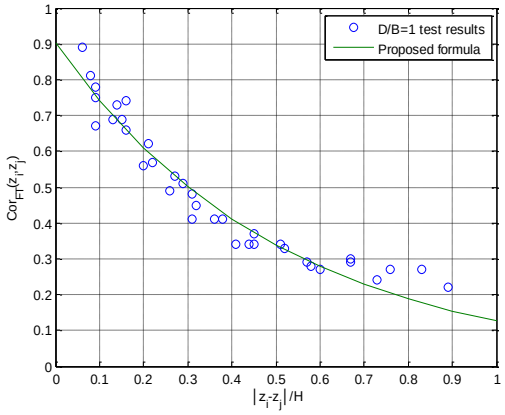

(c) *D*/*B*=1

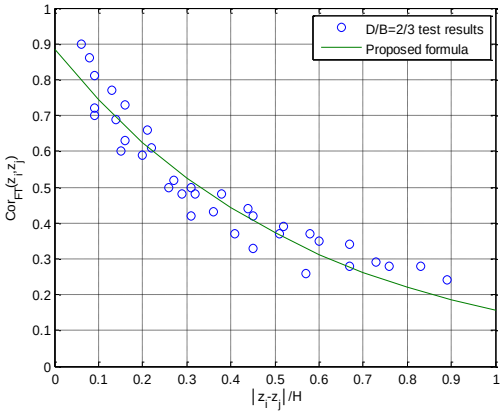

(d) *D*/*B*=0.67

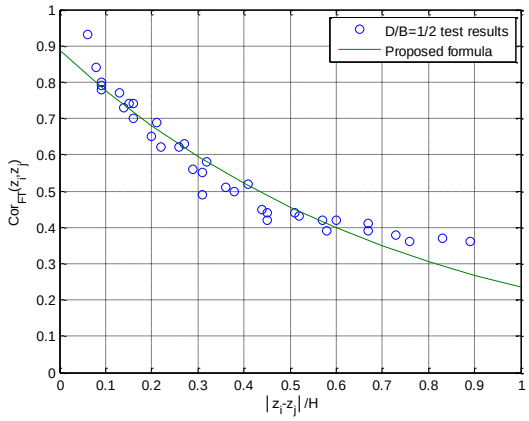

(e) *D*/*B*=0.5

Fig. 8 Vertical correlation coefficients of different models

Fig. 9 Models in wind tunnel

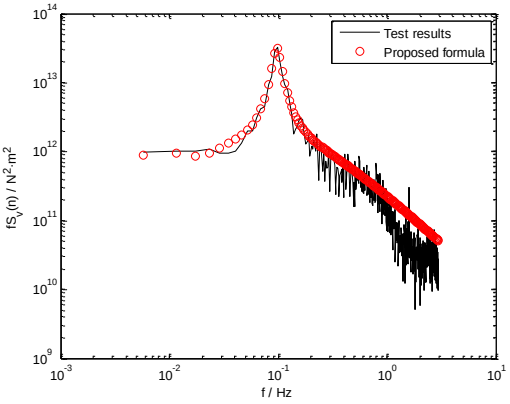

Fig. 10 Spectrum of generalized torque at the base

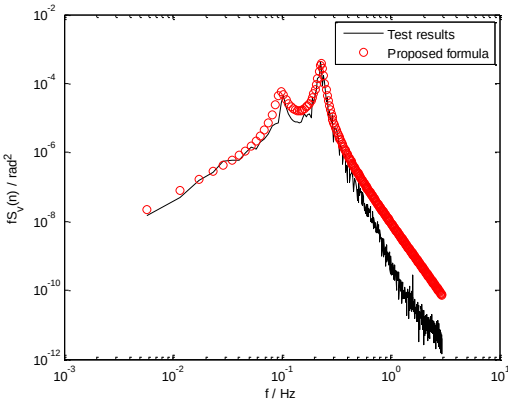

Fig. 11 Torsional response spectrum of angular displacement at the top of building

4. Example

Torsional wind loads and wind-induced response can not be evaluated accurately for lacking of theoretical formulas. Based on the above formulas proposed from the test results and the theoretical derivation in Appendix, a simplified expression is proposed to evaluate torsional wind loads and wind-induced response. Meanwhile, a practical project is illustrated to verify the accuracy of the expression.

The practical project is a super high-rise building made of reinforced concrete. The height of building is almost 260m, the cross section dimension B×D is 49.8 m×39.0 m.The damping ratio is supposed to be 5%. According to the terrain belongs to the building, exposure category C is chosen to design the building in finite element analysis. The first-order torsional frequency obtained from the analysis is 0.231 Hz. Scale models of 1:300 were conducted wind tunnel test to measure its wind loads and wind-induced response as shown in Fig. 9. The reference mean velocity at the top of model is 10 m/s. It should be pointed out that surrounding buildings make little influence on global wind loads of the main building for their insufficient height and dispersive distribution.

Spectrum of generalized torque at the base and spectrum of wind-induced torsional response at the top of building is respectively shown in Fig. 10 and Fig. 11. Since the side ratio is almost 0.783, narrow-band peak emerges in the spectrum of generalized torque at base with the reduced frequency of 0.098. Two peaks appear in spectrum of wind-induced torsional angular displacement at the top of building. The first peak is relevant to generalized torque, of which the reduced frequency keeps the same. The second peak is caused by the resonance component at the torsional nature frequency of building. Both of the two spectrums fitted by the proposed formula agree well with the test results at low frequency we concerned most, indicating the simplified expression can effectively evaluate torsional wind loads and wind-induced response.

5. Conclusions

Based on the extensive wind tunnel test on five rectangular models with different side ratios, this study investigated the characteristics of torsional wind loads on rectangular tall buildings in urban terrain. Comparisons of the results between the proposed formulas and the wind tunnel test results or literatures are made to verify the accuracy and the reliability of the proposed formulas, a practical project has also been illustrated to test the effectiveness of the simplified expression. The main conclusions obtained from this study are as follows:

(1) When $D/B \leq 1$, the RMS torque coefficients decrease as the model height increases; When $1 < D/B \leq 2$, the RMS torque coefficients first increase and then decrease as the model height increases.

(2) The RMS coefficients of base torsional moment first decreases with the side ratio up to 1.0, then increases as the side ratio increases from 1.0 to 2.0. When the side ratio $D/B \leq 1$, the RMS coefficients of base torsional moment are almost larger than the AIJ or GBJ proposed, to which designers should pay more attention.

(3) Base torque spectra varied with reduced frequency is almost the same as the torque spectra of each layer at different side ratio. When $D/B < 2$, there is a narrow-band peak in the torque spectra, of which the corresponding reduced frequency is lower than Strouhal number of rectangular buildings. Turbulence from windward and vortex shedding on the leeward side are the main contribution to the dynamic torque. When $D/B \geq 1$, energy of vortex shedding from the leeward and windward of side wall weakened, the Strouhal number component reduced. There are two peaks in the torque spectra which are caused by vortex shedding and reattachment of separated flow on the lee side of the side wall. As the side ratio D/B continues to increase, the first peak value decreases and the second peak value increases, and the reduced frequencies corresponding to the peaks approach to each other.

(4) Based on the linear-mode shape assumption, base torque spectrum acquired from HFBB keeps almost the same with those obtained from the pressure measurement. The proposed formulas of base torque spectrum on the basis of quasi-steady assumption as well as Marukawa's empirical expressions can well fit the test results.

(5) Vertical correlation coefficients are functions of side ratio and decrease exponentially as the relative height increases. When $D/B < 1$, correlation coefficients of the adjacent layers at upper half stay around 0.3~0.4. When $D/B > 1$, correlation coefficients of the adjacent layers rapidly decrease as the relative height increases.

(6) Both the Spectrum of generalized torque at the base and spectrum of wind-induced torsional response at the top of building fitted by the simplified expression agree well with the test results at low frequency. Therefore, the simplified expression in this study is available to estimate torsional

dynamic loads and wind-induced response for rectangular tall buildings in urban terrain.

Acknowledgments

The work described in this paper was fully supported by a grant from National Nature Science Foundation of China (Project no.51178179) and a grant from the Research Grants Council of Hong Kong Special Administrative Region, China (Project no. CityU 117709). The authors would like to thank the reviewers for their helpful comments.

References

AIJ Recommendations for Loads on Buildings (2004), Architectural Institute of Japan, Tokyo, Japan.

Boggs, D.W., Hosoya, N. and Cochran, L. (2000), "Sources of torsional wind loading on tall buildings: Lessons from the wind tunnel", *Proceedings of the 2000 Structure Congress & Exposition*, Philadelphia, May.

Davenport, A.G. (1967), "Gust loading factors", *J. Struct. Div*. ASCE., **93**(3), 11-34.

Davenport, A.G. (1995), "How can we simplify and generalize wind loads", *J. Wind Eng. Ind. Aerod.*, **54/55**, 657-669.

GB50009-2012 (2012), Load Code for the Design of Building Structures, China Architecture & Building Press, Beijing.

Gu, M., Tang, Y. and Quan, Y. (2009), "Basic characteristics of torsional fluctuating wind force of rectangular tall buildings", *J. Build. Struct.*, **30**(5), 191-197. (in Chinese)

Ha, Y.C., Kim, Y.S. and Kim, H.R. (2008), "Fluctuating torsional moment coefficient and power spectral density coefficient for estimating wind loadings on a tall building", *Proceedings of the 4th International Conference on Advance in Wind and Structures.*, Jeju, May.

Isyumov, N. and Poole, M. (1983), "Wind induced torque on square and rectangular building shapes", *J. Wind Eng. Ind. Aerod.*, **13**,183-196.

Kareem, A. (1981), "Wind induced torsional loads on structures", *Eng. Struct.*, **3**, 85-86.

Kareem, A. (1982), "Across wind response of buildings", *J. Struct. Div.*, ASCE, **108**(4), 869-887.

Katagiri, J., Ohkuma, T., Marukawa, H. and Tsurumi, T. (2006), "Characteristics of fluctuating torsional moment acting on rectangular high-rise buildings", *Proceedings of the 19th National Symposium on Wind Engineering*, Tokyo, December.

Kwon, D.K., Tracy, K.C. and Kareem, A. (2008), "e-Analysis of high-rise buildings subjected to wind loads", *J. Struct. Eng.*, ASCE, **134**(7), 1139-1153.

Li, Q.S. (2000), "Evaluation of wind-induced vibration of tall buildings and reliability analysis: a case study", *Tran. H.K. Ins. Eng.*, **7**(1), 47-50.

Liang, S.G., Li, Q.S., Liu, S.C., Zhang, L.L. and Gu, M. (2004), "Torsional dynamic wind loads on rectangular tall buildings", *Eng. Struct.*, **26**(1), 129-137.

Lin, N., Letchford, C., Tamura, Y., Liang, B. and Nakamura, O. (2005), "Characteristics of wind forces acting on tall buildings", *J. Wind Eng. Ind. Aerod.*, **93**(3), 217-242.

Marukawa, H., Ohkuma, T. and Momomura, Y. (1992), "Across wind and torsional acceleration of prismatic high rise buildings", *J. Wind Eng. Ind. Aerod.*, **42**(1-3), 1139-1150.

Marukawa, H and Ohkuma, T. (1996), "Formula of fluctuating wind forces for estimation of across-wind and torsional response of prismatic high rise building", *J. Struct. Constr. Eng. Jap*, **482**, 33-42.

Saunders, J.W. and Melbourne, W.H. (1975), "Tall rectangular building response to cross-wind excitation", *Proceedings of the Fourth International Conference on Wind Effects on Buildings and Structures*, London, September.

Tallin, A. and Ellingwood, B. (1984), "Serviceability limit states: wind induced vibrations", *J. Struct. Eng.*, ASCE, **110**(10), 2424-2437.
Tallin, A. and Ellingwood, B. (1985), "Analysis of torsional moments on tall buildings", *J. Wind Eng. Ind. Aerod.*, **18**(2), 191-195.
Tang, Y. (2006), "Research on the wind excited vibrations and static-equivalent wind loads of torsionally coupled high-rise buildings", Ph.D. Dissertation, Tongji University, Shanghai.
Tang, Y., Gu, M. and Quan, Y. (2009), "Mathematical model of torsional fluctuating wind force on rectangular tall buildings", *J. Build. Struct.*, **30**(5), 198-204. (in Chinese)
Zhou, Y., Kijewski, T. and Kareem, A. (2003), "Aerodynamic loads on tall buildings: Interactive database", *J. Struct. Eng.*, ASCE, **129**(3), 394-404.

Appendix. Evaluation of wind-induce torsional response on rectangular tall buildings

Wind-induce torsional response on rectangular tall buildings can be effectively evaluated on basis of the following assumptions:

(1) Imaginary component of the cross power spectrum contributes little to cross spectral density of torsional wind loads.

(2) Non-dimensional spectrum of base torque is consistent with those of different layers.

(3) Vertical coherence function is equivalent to vertical correlation coefficient, both of which are functions irrelevant with frequency.

(4) The proposed formulas about RMS torque coefficients, power spectrum density of torsion as well as vertical torsional correlation coefficient are available to apply in the expression derivation.

According to the knowledge of structure dynamics and theory of random vibration, the cross spectrum density of wind loads for different height can be calculated by the following expressions

$$S_{F_T}(z_i, z_j; f) = \sqrt{S_{F_T}(z_i; f) S_{F_T}(z_j; f)}\, Coh_{F_T}(z_i, z_j) = \sigma_{F_T}(z_i)\sigma_{F_T}(z_j) \sqrt{\frac{S_{F_T}(z_i; f)}{\sigma^2_{F_T}(z_i)} \frac{S_{F_T}(z_j; f)}{\sigma^2_{F_T}(z_j)}}\, Cor_{F_T}(z_i, z_j) \tag{19}$$

where $S_{F_T}(z_i; f)$, $S_{F_T}(z_j; f)$ are respectively auto spectrums of wind loads at the height of z_i and z_j ; $Coh_{F_T}(z_i, z_j)$ is correlation coherence of wind loads from the height of z_i and z_j, $Cor_{F_T}(z_i, z_j)$ is vertical correlation coefficient.

Based on the second assumption, $\frac{S_{F_T}(z_i; f)}{\sigma^2_{F_T}(z_i)}$ is equal to $\frac{S_{F_T}(z_j; f)}{\sigma^2_{F_T}(z_j)}$, we can regard that

$$S'_{F_T}(f) = \frac{S_{F_T}(z_i; f)}{\sigma^2_{F_T}(z_i)} = \frac{S_{M_T}(f)}{\sigma^2_{M_T}} \tag{20}$$

Therefore, Eq. (20) can be simplified as

$$S_{F_T}(z_i, z_j; f) = \sigma_{F_T}(z_i)\sigma_{F_T}(z_j) S'_{F_T}(f) Cor_{F_T}(z_i, z_j) \tag{21}$$

In the light of structure dynamics, the *k*th generalized force spectrum can be expressed as

$$S^*_{F_k}(f) = \int_0^H \int_0^H S_{F_T}(z_i, z_j; f) \varphi_k(z_i) \varphi_k(z_j) dz_i dz_j \tag{22}$$

in which, $\varphi_k(z_i)$, $\varphi_k(z_j)$ are the *k*th mode shapes at the height of z_i and z_j.

When taking the Eq. (20) into the Eq. (22) and combining the Eq. (1), the *k*th generalized force spectrum is simplified as follows

$$S^*_{F_k}(f) = \frac{(0.5\rho U_H^2)^2 L_i L_j B^4 S_{M_T}(f)}{\sigma^2_{M_T}} \times \int_0^H \int_0^H C_{F_T}(z_i) C_{F_T}(z_j) Cor_{F_T}(z_i, z_j) \varphi_k(z_i) \varphi_k(z_j) dz_i dz_j \tag{23}$$

Where the formulas about $\frac{S_{M_T}(f)}{\sigma^2_{M_T}}$, $C_{F_T}(z)$ and $Cor_{F_T}(z_i, z_j)$ have been proposed in the study.

Regarding the theory of random vibration, the *kth* fluctuating displacement response spectrum is

$$S^*_{Y_k}(f) = \frac{S^*_{F_k}(f)}{M_k^2}\left|H_k(f)\right|^2 \tag{24}$$

In which, $M_k = \int_0^H m(z_i)\varphi_k(z_i)dz_i$ is the *k*th generalized mass of buildings.

$\left|H_k(f)\right|^2 = \frac{1}{(2\pi n_j)^4\left\{\left[1-(\frac{n}{n_j})^2\right]^2 + (2\varsigma_j\frac{n}{n_j})^2\right\}}$ represents the *k*th frequency response function.

The fluctuating displacement response is thought to be zero mean stationary random process, therefore, the *k*th RMS angular displacement can be integrated as

$$\sigma_{Y_k} = \sqrt{\int_0^\infty S^*_{Y_k}(f)df} \tag{25}$$